archives
of thermodynamics
Vol. **38**(2017), No. 4, 89–107
DOI: 10.1515/aoter-2017-0026

The influence of stack position and acoustic frequency on the performance of thermoacoustic refrigerator with the standing wave

JAKUB KAJUREK*
ARTUR RUSOWICZ
ANDRZEJ GRZEBIELEC

Warsaw University of Technology, Institute of Heat Engineering, Nowowiejska 21/25, 00-665 Warszawa, Poland

Abstract Thermoacoustic refrigerator uses acoustic power to transport heat from a low-temperature source to a high-temperature source. The increasing interest in thermoacoustic technology is caused due to its simplicity, reliability as well as application of environmentally friendly working fluids. A typical thermoacoustic refrigerator consists of a resonator, a stack of parallel plates, two heat exchangers and a source of acoustic wave. The article presents the influence of the stack position in the resonance tube and the acoustic frequency on the performance of thermoacoustic refrigerator with a standing wave driven by a loudspeaker, which is measured in terms of the temperature difference between the stack edges. The results from experiments, conducted for the stack with the plate spacing 0.3 mm and the length 50 mm, acoustic frequencies varying between 100 and 400 Hz and air as a working fluid are consistent with the theory presented in this paper. The experiments confirmed that the temperature difference for the stack with determined plate spacing depends on the acoustic frequency and the stack position. The maximum values were achieved for resonance frequencies and the stack position between the pressure and velocity node.

Keywords: Thermoacoustic; Thermoacoustic refrigerator; Stack position; Acoustic frequency

*Corresponding Author. Email: jakub.kajurek@itc.pw.edu.pl

Nomenclature

a	–	speed of sound, m/s
A	–	cross-sectional area, m^2
BR	–	blockage ratio
c_p	–	isobaric heat capacity, J/(kg K)
c_s	–	heat capacity of the stack plates, J/(kg K)
DR	–	drive ratio
f	–	frequency, Hz
i	–	imaginary unit
$\dot{H}$	–	energy flux, W
k	–	wave number, 1/m
K	–	thermal conductivity, W/(m K)
l	–	half of the plate thickness, m
L	–	length, m
p	–	pressure, Pa
Pr	–	Prandtl number
$\dot{Q}$	–	heat flux, W
s	–	entropy, J/(kg K)
t	–	time, s
T	–	temperature, K
u	–	velocity in x direction, m/s
w	–	velocity in y direction, m/s
$\dot{W}$	–	acoustic power, W
y_0	–	half of the plate spacing, m
x	–	longitudinal coordinate to acoustic wave propagation direction, m
y	–	perpendicular coordinate to acoustic wave propagation direction, m

Greek symbols

β	–	thermal expansion coefficient, 1/K
δ_k	–	thermal penetration depth, m
δ_v	–	viscous penetration depth, m
ϵ_s	–	plate heat capacity ratio
Γ	–	normalized temperature gradient
κ	–	ratio, isobaric to isochoric specific heats
λ	–	wavelength, m
π	–	perimeter, m
ρ	–	density, kg/m^3
ω	–	angular frequency, rad/s

Superscripts

A	–	amplitude
c	–	center
$crit$	–	critical
m	–	mean
n	–	normalized
s	–	solid or standing
1	–	fluctuating part

1 Introduction

In recent years the environmental aspects of refrigeration systems have become more important. Hence, the current interests of researchers focus on the development of alternative technologies, which will be able to replace solutions based on hazardous refrigerants. One of the most promising approach in the field of the alternative cooling systems is the thermoacoustic refrigeration [1]. Other solutions include adsorption and the absorption devices [2,3].

The theory of thermoacoustic includes all the effects in which heat and acoustic energy are transported together or mutually transformed [4]. The devices that convert heat to acoustic energy are called thermoacoustic engines, and the devices that use acoustic energy to transport heat from a low-temperature source to a high-temperature source are called thermoacoustic refrigerators [5]. The increasing interest in the thermoacoustic technology is not only due to its environmentally friendly working fluids, but also because of its simplicity and reliability – the thermoacoustic devices have no moving components and sliding seals [6]. Despite many advantages of the thermoacoustic technology, it has still not reached technical maturity. The thermoacoustic refrigerators, as a result of lower efficiency than the commercial refrigerators, are not yet competitive. They achieve 10 to 20% of Carnot efficiency as opposed to 33 to 50% for conventional solutions [7]. Thus, many efforts are taken to improve and optimize the design and the performance of the thermoacoustic devices.

The paper investigates the influence of stack position in the resonance tube and the acoustic frequency on the performance of standing wave thermoacoustic refrigerator. Nine different stack positions at four frequencies were examined in terms of temperature difference across the stack ends at a prototype device driven by a loudspeaker and air as a working fluid, assembled for experimental setup. Besides the results and conclusions presented in last paragraphs, the basis of the thermoacoustic theory and construction of the thermoacoustic refrigerators are also discussed in this paper.

2 Thermoacoustic theory

The thermoacoustic devices include two thermodynamic media: an oscillating fluid and a solid, such as a thin plate [8]. The plate introduced into the oscillating fluid, because of the heat transfer with the fluid, modifies the

original temperature oscillations caused by the acoustic wave, both in magnitude and in phase, about a thermal penetration depth $\delta_k = \sqrt{K/(\rho_m c_p \omega)}$ away from the plate. Therefore, in the fluid the heat can be transported in parallel to the plate and acoustic power can be absorbed or produced [5].

2.1 Thermodynamic cycle

The thermodynamic cycle of thermoacoustic devices can be explained by considering a solid plate aligned in the direction of acoustic standing wave, with imposed mean-temperature gradient ∇T_m along the plate. Because of the acoustic wave the gas parcel near the plate experiences changes in pressure, velocity and temperature. On the one hand the temperature changes of gas parcel comes from its adiabatic compression and expansion by acoustic wave, on the other, it is a result of heat transfer between the plate and the fluid. The heat flow between these two media creates a time delay in temperature oscillation, which is needed to realize a thermodynamic cycle by the fluid parcels [5]. But not every parcel is driven through the thermodynamic cycle. Those, which are far from the plate have no thermal contact and are simply compressed and expanded adiabatically by acoustic wave, while the parcels that are too close the plate have a very good thermal contact and are simply compressed and expanded isothermally. The elements of fluid, at about a distance of a thermal penetration depth from the plate, have enough of good thermal contact (imperfect thermal contact) to exchange some heat, and thus create a time delay between heat transfer and the motion [9].

Whether the plate works as a refrigerator or as an engine depends on the magnitude of the mean temperature gradient imposed on the plate relative to a critical temperature gradient, defined as [5]

$$\nabla T_{crit} = T_m \frac{\beta \omega p_1}{\rho_m c_p u_1^s} \,. \tag{1}$$

The critical temperature gradient is a value for which the temperature change due to adiabatic compression and expansion matches the temperature change due to parcel's motion along the plate with given mean temperature gradient ∇T_m. For $\nabla T_m < \nabla T_{crit}$ the acoustic energy is absorbed, and the heat is transported in the mean temperature gradient direction (refrigerator cycle). For $\nabla T_m > \nabla T_{crit}$ the acoustic energy is generated by utilizing heat flowing against the mean temperature gradient (engine cycle) [10].

The refrigeration cycle of a fluid parcel in the thermoacoustic refrigerator is shown in Fig. 1. To keep things simple, the acoustic wave is considered as a square wave. In the first step, under the influence of standing wave, the fluid parcel is compressed adiabatically, moves towards the pressure antinode and increases in temperature by an amount $2T_1$. After the displacement, the fluid parcel is warmer than the plate, so in the second step heat flows irreversibly at constant pressure from the parcel to the plate. In the third step, the fluid parcel moves back to its initial position, expands and cools down adiabatically. After the displacement in opposite direction the fluid parcel is colder than the plate, and in the fourth step irreversible constant pressure heat transfer from the plate towards the fluid parcel takes place. The fluid parcel after this process reached its initial parameters, so also completed the thermodynamic cycle.

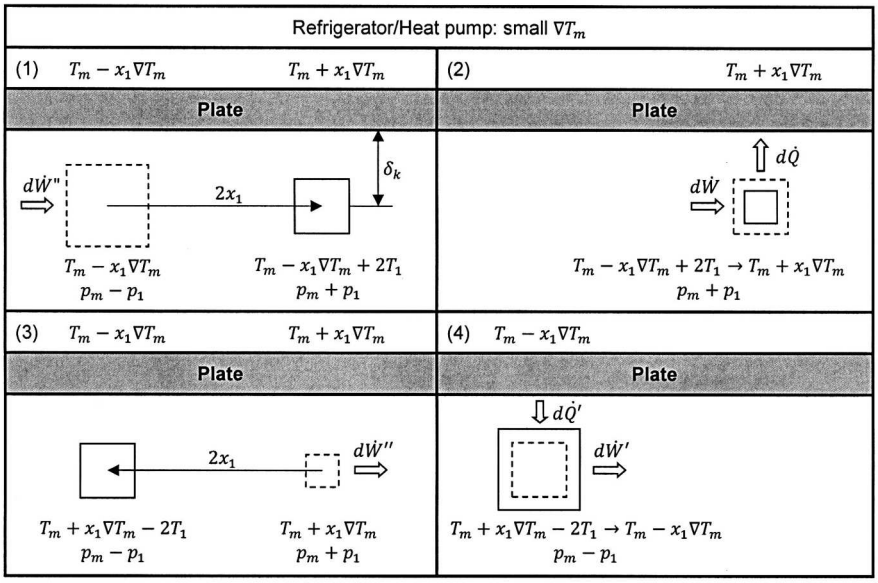

Figure 1: Thermodynamic cycle of the fluid parcel in a thermoacoustic refrigerator.

In most cases the length of the plate is larger than the displacement of given fluid parcel. Thus, the heat from one end of the plate to the other is transported by a series of fluid parcels (Fig. 2). During the first part of refrigeration cycle each parcel moves towards pressure antinodes and leaves at its maximum displacement an amount of heat. During the second half

of the same cycle, the parcels moves backs to their starting position and pick up from the plate the same amount of heat, which was deposited there a half cycle earlier by the adjacent parcel. In effect, the heat is transferred from one end to the other by gas parcels as bucket bridge and the plate is used only for the temporary storage of heat [6].

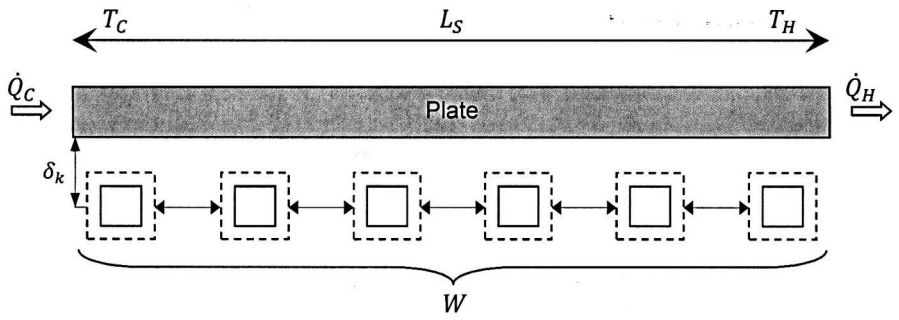

Figure 2: Heat transfer by the gas parcels along the stack plate, $\dot{Q}_c$, $\dot{Q}_H$ – cold-side and hot-side heat flux.

2.2 Mathematical model

The heat flux transported along the single plate under ordinary circumstances is small. However, in typical devices the entire cross section of the standing wave is filled by the parallel plates, and thus high heat fluxes can be easily achieved. The simplified model of the stack is considered with the following assumptions [5,7,11]:

- theory is linear, second-order effects other than energy transport, such as acoustic streaming are neglected;
- plate is perfectly rigid and stationary;
- plates have the thicknesses $2l$ and spacing $2y_0$ (Fig. 3);
- temperature spanned along the stack is much smaller than the absolute temperature and thus the thermophysical properties of the fluid can be assumed independent of coordinate longitudinal to the acoustic wave propagation direction (x);
- length of the stack plates is much shorter than wavelength (short stack approximation) and hence the pressure and parcel velocities can be

considered constant along the stack and the stack does not affect the acoustic standing wave;

- ratio between half the plate spacing y_0 and the thermal penetration depth δ_k is much greater than one (boundary layer approximation), which causes that the complex hyperbolic tangents, which arise in the solution of the short boundary layer approximation can be set to unity;
- mean fluid velocities are zero;
- acoustic amplitudes are assumed low enough to avoid turbulence;
- all variables oscillate at angular frequency ω:

$$p = p_m + p_1(x)e^{i\omega t} \,, \tag{2}$$

$$\rho = \rho_m(x) + \rho_1(x,y)\, e^{i\omega t} \,, \tag{3}$$

$$\overrightarrow{v}_1 = \overrightarrow{x}\, u_1(x,y)\, e^{i\omega t} + \overrightarrow{y}\, w_1(x,y)\, e^{i\omega t} \,, \tag{4}$$

$$T = T_m(x) + T_1(x,y)\, e^{i\omega t} \,, \tag{5}$$

$$T_s = T_m(x) + T_{s1}(x,y)\, e^{i\omega t} \,, \tag{6}$$

$$s = s_m(x) + s_1(x,y)e^{i\omega t} \,, \tag{7}$$

where the terms with the subscript m denote the mean value and with the subscript '1' the fluctuating part of the individual variables. With these approximations, the standing wave acoustic pressure and velocity can be written as [5]:

$$p_1 = p_A \sin(kx) \,, \tag{8}$$

$$u_1 = i\left(1 + \frac{l}{y_0}\right)\left(\frac{p_A}{\rho_m a}\right)\cos(kx) = iu_1^s \,. \tag{9}$$

The expressions for energy flux and acoustic power in the stack of thermoacoustic devices, derived from the time average equations of continuity, motion and energy, are described as [5]:

$$\begin{aligned}\dot{H} = &-\frac{1}{4}\pi\delta_k \frac{T_m\beta p_1 \langle u_1^s\rangle}{(1+\epsilon_s)(1+\mathrm{Pr})\left(1-\frac{\delta_v}{y_0}+\frac{\delta_v^2}{2y_0^2}\right)} \\ &\times\left[\Gamma\frac{1+\sqrt{\mathrm{Pr}}+\mathrm{Pr}+\mathrm{Pr}\epsilon_s}{1+\sqrt{\mathrm{Pr}}}-\left(1+\sqrt{\mathrm{Pr}}-\frac{\delta_v}{y_0}\right)\right] \\ &-\Pi(y_0K + lK_s)\frac{dT_m}{dx} \,,\end{aligned} \tag{10}$$

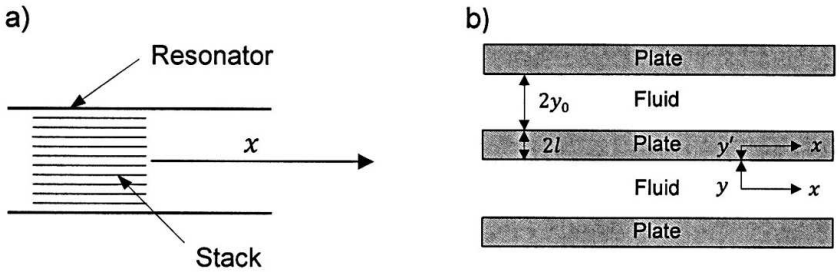

Figure 3: Stack geometry: a) overall view, b) expanded view.

$$\dot{W} = \frac{1}{4}\Pi_k \triangle x \frac{(\kappa-1)\,\omega p_1^2}{\rho_m a^2\,(1+\epsilon_s)} \times \left(\frac{\Gamma}{\left(1+\sqrt{\mathrm{Pr}}\right)\left(1-\frac{\delta_v}{y_0}+\frac{\delta_v^2}{2y_0^2}\right)} - 1 \right)$$
$$-\frac{1}{4}\Pi_v \triangle x \frac{\delta_m \langle u_1^s \rangle^2}{1-\frac{\delta_v}{y_0}+\frac{\delta_v^2}{2y_0^2}}\,, \tag{11}$$

where $\langle u_1^s \rangle$ is the mean velocity in x direction defined as $\langle u_1 \rangle = \frac{1}{y_0}\int_0^{y_0} u_1 dy = i\,\langle u_1^s \rangle$, Γ is the normalized temperature gradient described as $\Gamma = \nabla T_m / \nabla T_{crit}$ and ϵ_s is the plate heat capacity ratio expressed as $\epsilon_s = \sqrt{K\rho_m c_p / (K_s \rho_s c_s)}$. The first term in energy flux (10) describes the heat flux transported due to the thermoacoustic effect, the second term is just the ordinary conduction of heat down the temperature gradient by the fluid and solid [5].

The Eqs. (10) and (11) indicate that there are 18 independent parameters, which influence the performance of the thermoacoustic devices. These parameters can be divided into three groups [7]:

- Design and operational requirements of thermoacoustic device, such as desired cooling or acoustic power, acoustic frequency, mean pressure and mean temperature, pressure amplitude and temperature gradient imposed on the stack.
- Material related variables, which describe the thermophysical properties of the working fluid and the stack plates.

- Geometry design parameters like plate thickness or spacing.

The number of independent parameters from Eqs. (10)–(11) can be reduced through normalization. The normalized energy flux with neglected heat conduction, both in the plate and fluid, and normalized acoustic power are given as [12]:

$$\dot{H}_n = -\frac{1}{8\kappa}\delta_{kn}(\mathrm{DR})^2\frac{\sin(2x_{cn})}{(1+\mathrm{Pr})\,\Lambda}\left[\Gamma\frac{1+\sqrt{\mathrm{Pr}}+\mathrm{Pr}}{1+\sqrt{\mathrm{Pr}}}-(1+\sqrt{\mathrm{Pr}}-\sqrt{\mathrm{Pr}}\delta_{kn})\right] \tag{12}$$

$$\dot{W}_n = \frac{1}{4\kappa}\delta_{kn}(\mathrm{DR})^2 L_{sn} \times\left[\mathrm{BR}\,(\kappa-1)\cos^2(x_{cn})\left(\frac{\Gamma}{1+\sqrt{\mathrm{Pr}}}-1\right)-\frac{\sin^2(x_{cn})\sqrt{\mathrm{Pr}}}{\mathrm{BR}\Lambda}\right], \tag{13}$$

where

$$\Lambda = 1-\delta_{kn}\sqrt{\mathrm{Pr}}+\frac{1}{2}\mathrm{Pr}\delta_{kn}^2\,. \tag{14}$$

The normalized parameters are equal:

$$\Gamma=\frac{\nabla T}{\nabla T_{crit}}=\frac{\Delta T_{mn}\tan(x_{cn})}{\mathrm{BR}(\kappa-1)L_{sn}}\,,\qquad \delta_{kn}=\frac{\delta_k}{y_0}\,,$$
$$\mathrm{DR}=\frac{p_1}{p_m}\,,\qquad \delta_{vn}=\frac{\delta_v}{y_0}\,,$$
$$\dot{H}_n=\frac{\dot{H}}{p_m a A}\,,\qquad L_{sn}=k\triangle x\,,$$
$$\dot{W}_n=\frac{\dot{W}}{p_m a A}\,,\qquad x_{cn}=kx\,,$$
$$\Delta T_{mn}=\frac{\Delta T_m}{T_m}\,,\qquad \mathrm{BR}=\frac{y_o}{(y_0+l)}\,.$$

3 Thermoacoustic refrigerators

3.1 Classification

Thermoacoustic refrigerators can be categorized depending on the phase shift between the pressure and velocity oscillations in acoustic wave [13]. For a pure standing-wave the pressure and velocity oscillations are $\pi/2$

out of phase, while for a travelling wave are in phase. Therefore, the simple straight-line resonator such as closed-closed $\lambda/2$ or a closed-open $\lambda/4$ tube is needed to provide necessary acoustic environment for standing wave (Fig. 4a), and looped tube for travelling wave (Fig. 4b).

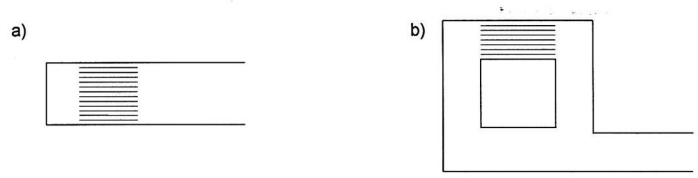

Figure 4: Schematic illustrations of resonator configurations: a) for standing wave, b) for travelling wave.

Another classification of the thermoacoustic refrigerators can be based on the source of acoustic wave. If the acoustic energy is delivered from the thermoacoustic engines, the devices are called thermoacoustically-driven thermoacoustic refrigerators. While, if the acoustic energy is provided by an acoustic driver, for example a loudspeaker, the devices are called acoustically-driven thermoacoustic refrigerators [6].

3.2 Construction

A schematic illustration of the acoustically-driven thermoacoustic refrigerator with standing wave is shown in Fig. 5. The device consists of parts such as an acoustic driver, a stack, a resonator, the heat exchangers and a working fluid.

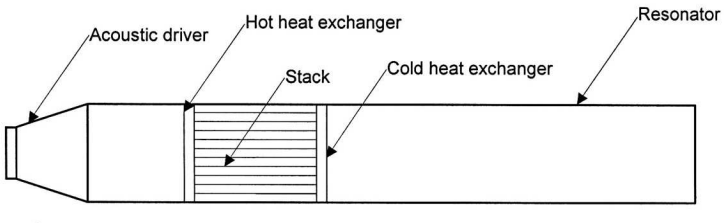

Figure 5: Schematic illustration of the standing wave thermoacoustic refrigerator with an acoustic driver.

3.2.1 Acoustic driver

The acoustic driver generates an acoustic wave with determined frequency and pressure amplitude. Commercial, moving-coil loudspeakers with wide range of frequencies are widely used. They are cheap, compact and can be easily adapted to the thermoacoustic refrigerators. But they have also one important disadvantage – low efficiency, which decreases the overall efficiency of the device. Thus, many drivers are modified to reduce the losses [12,14,15].

3.2.2 Heat exchangers

The heat exchangers in the thermoacoustic refrigerator are needed to supply heat from a low-temperature reservoir to cold end of the stack and extract heat from the hot end of the stack to a high-temperature reservoir. They should provide high heat transfer coefficients and low dissipation of acoustic power. Three types of heat exchangers are suitable for thermoacoustic refrigerators: parallel-strips, finned-tubes, and flat-tube-banks [16]. The maximum length of heat exchanger should be roughly two times the fluid parcel displacement [5].

3.2.3 Stack

The stack is the most important part of the thermoacoustic refrigerator, in which the heat-pumping process takes place. There are many different stack geometries: parallel plates, circular pores, pin arrays, triangular pores [12]. The main objective for stack geometry selection is to increase the thermal boundary layer surrounding the solid wall where the thermoacoustic effect could occur [17]. The optimal stack spacing for the parallel plates is between $2\delta_k$ to $4\delta_k$, where δ_k is the thermal penetration depth [14,15]. The stack length must meet the short stack approximation. For given operation parameters the maximum length exists, above which performance starts to decrease [7]. The stack material should minimize the losses caused by the ordinary heat conduction along the temperature gradient [5]. The most commonly used material for the stack is Mylar [12,14,15]. Typically, the stack is located closer to the pressure antinode than the pressure node. The optimal location depends on the viscous and thermal relaxation losses [17]. The optimal stack centre position proposed by Swift is $\lambda/20$ measured away from the pressure antinode [18], whereas the value postulated by Tijani it is

$\lambda/8$ [12]. In most of other experiments the optimum position falls between these two quantities [17].

3.2.4 Resonator

The resonance tube encloses heat exchangers, the stack, acoustic driver and the working fluid. The length of resonator is determined by resonance frequencies, in most cases the tubes are the quarter wave length or half wave length. The simplest and most appropriate geometry of the resonance tube is cylinder [7], but rectangular geometries are also used [19,20]. The resonator material should have large acoustic impedance to minimize the losses in acoustic wave [20].

3.2.5 Working fluid

The working fluid properties play an important role in determining cooling power and efficiency. The best working fluids for the thermoacoustic refrigerators have high ratios of specific heat and low Prandtl number [21]. These properties are sometimes optimized by using a binary mixture of helium and other noble gases [22]. In experiments related with the thermoacoustic devices air is widely used because of its availability [17].

4 Experimental setup

The schematic illustration of experimental apparatus, which let only measure the temperature across the stack, is shown in Fig. 6. It consists of the loudspeaker, the resonator, the stack, the amplifier, sound generator and measuring devices. The refrigerator has no heat exchanger at the ends of the stack, because the main aim of the experiment is to examine temperature difference across the stack ends under various operating conditions – stack positions and acoustic frequencies.

The loudspeaker constitutes the acoustic wave source. It has a frequency in the range of 40–500 Hz, 200 W RMS continuous power and 4 Ω nominal impedance. The loudspeaker is excited by the amplifier fed with a sinusoidal signal, provided by the software installed on the computer. The amplifier has a frequency response in the range of 20–20000 Hz and distortion less than 0.01%. The resonance tube is rectangular with the inner dimensions 0.045 m x 0.045 m, length of 2 m and is filled with air at atmospheric pressure. One end of the resonator is connected to the loudspeaker, second

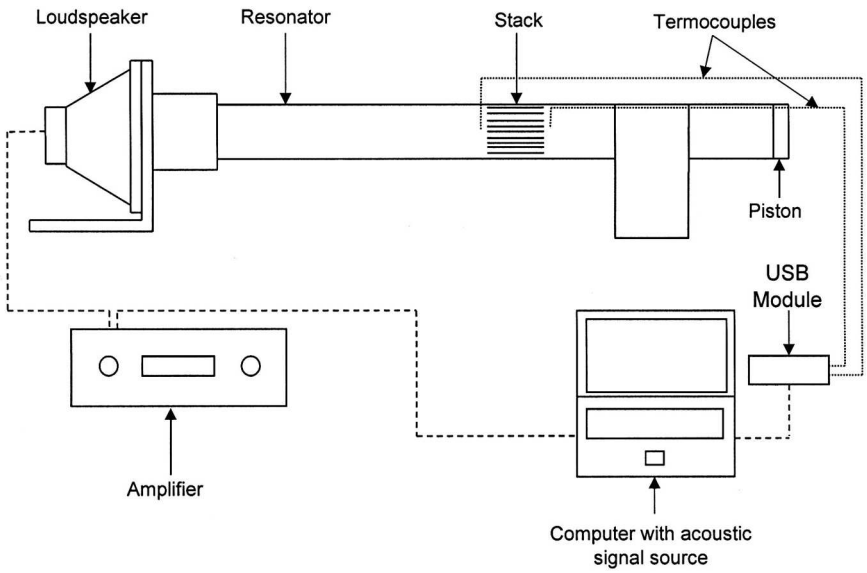

Figure 6: Schematic illustration of experimental apparatus.

is closed with the cork piston. The resonator length can be adjusted to the operating frequency by the change of piston position. The stack consists of parallel plates with dimensions 0.00178 m x 0.045 m x 0.05 m, which are spaced by the fishing line with 0.003 m thickness (Fig. 7). The plates are made from PET. The temperature difference across the stack is measured by the type-T thermocouples, which are connected to the USB module – data acquisition card. The value of the temperature for each end of the stack is then displayed by the special program installed on the computer, with the accuracy 0.1 K and is saved in the *.xlsx file.

The experiments were done at four different acoustic frequencies: 100, 200, 300 and 400 Hz, and nine different positions of the stack centre: $L_s/2$, $\lambda/16$, $\lambda/8$, $3\lambda/16$, $\lambda/4$, $5\lambda/16$, $3\lambda/8$, $7\lambda/16$, $\lambda/2$- $L_s/2$, where L_s is the stack length (50 mm) and λ is the acoustic wave length, for given frequency calculated based on equation:

$$\lambda = \frac{a}{f} \,. \tag{15}$$

The first and the last stack positions were limited by the resonator length, which in these measurements was equalled to the half-length of acoustic wave. The temperature difference was read, when the steady state was

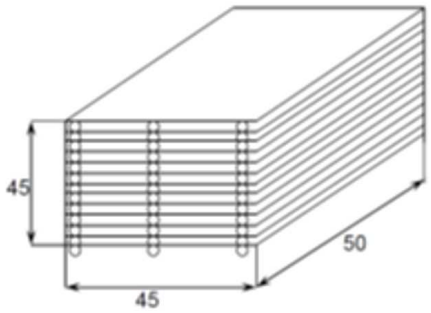

Figure 7: Schematic illustration of parallel plate stack.

achieved. Additionally, for determined resonator length, the influence of other frequencies than resonance – remaining three, was investigated (e.g., for resonator length corresponding to 100 Hz also for 200, 300, and 400 Hz).

5 Experimental results and discussion

The temperature differences between the stack ends as functions of stack position in the resonance tube at four resonance frequencies are shown in Fig. 8, where λ is the wave length for given frequency (100, 200, 300 or 400 Hz) and L_s is the stack length. For all frequencies, the dependence is close to the sinusoid, with the maximum values shifted toward the pressure antinode, which follow from the product DR$= p_1/p_m$ in Eq. (12). The maximum temperature difference for each frequency was achieved for the stack centre position at $\lambda/16$, while zero for $\lambda/4$, where λ is the pressure node at which heat flow vanishes (Eq. (12)). The temperature difference changes sign as the pressure gradient changes sign, however, for stack positions located further from the loudspeaker, behind the pressure node, the temperature differences are smaller than for the positions closer to the loudspeaker, for example $7\lambda/16$ versus $\lambda/16$, which is a consequence of acoustic power dissipation in the resonance tube.

Figure 8 indicates also that the temperature difference for the stack with determined length and plate spacing depends on acoustic frequency. The highest temperature difference is almost the same for 200 and 300 Hz, and is nearly equal to 16 K. The optimal frequency for investigated stack with 0.3 mm plate spacing should be between these two frequencies. The tem-

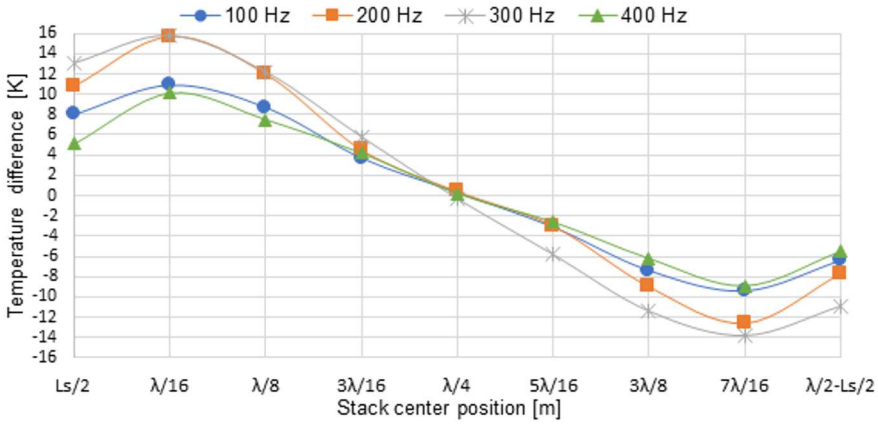

Figure 8: Temperature difference between stack ends versus stack position for resonance frequencies.

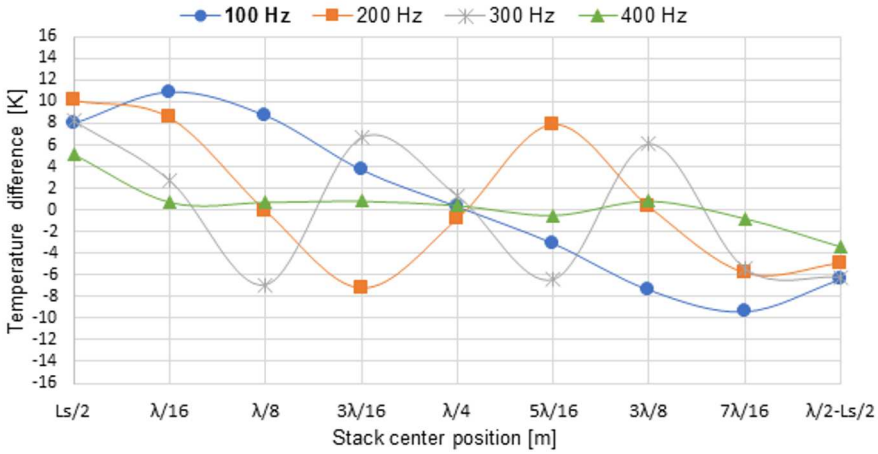

Figure 9: Temperature difference between stack ends versus stack position with main resonance frequency 100 Hz (λ is the wave length for 100 Hz).

perature differences for 100 and 400 Hz are lower than for 200 and 300 Hz. For 100 Hz, the thermoacoustic effect is reduced by the viscous losses. The plate spacing $2y_o$ is then around $1.6\delta_k$, where δ_k is the thermal penetration depth. This means also that for 100 Hz and plate spacing 0.3 mm the boundary layer approximation is not met (Sec. 2.2). For 400 Hz, the temperature distribution might be affected by the stack length.

The temperature differences across the stack for frequencies other than the resonance and resonator length other than the half-length of acoustic wave are shown in Figs. 9–12, where λ is the wave length of frequency bolded in given figure. In every case the highest temperature difference was achieved for resonator length corresponding to the half-length of acoustic wave.

Figure 9 presents the results for resonator length equal to: $\lambda/2$ for 100 Hz, λ for 200 Hz, 1.5λ for 300 Hz, and 2λ for 400 Hz. Every investigated frequency in this case is the resonance frequency. The temperature dependence of stack position is close to a sinusoid again, with zeros at both pressure and velocity nodes (or antinodes). For 400 Hz the positions, beyond first and last, are in the pressure or velocity node and thus the relation in Fig. 9 is partly linear. The maximum temperature differences obtained for 200 Hz and 300 Hz are close to the maximum temperature difference obtained for 100 Hz, but are much smaller than this presented in Fig. 8. The differences between the results depicted in Fig. 9 for 200 Hz and 300 Hz are caused partly by the increase in energy dissipation in the resonance tube, which is respectively two and three times longer, and partly by the change of the stack position relative to the position in the half-wave length resonator.

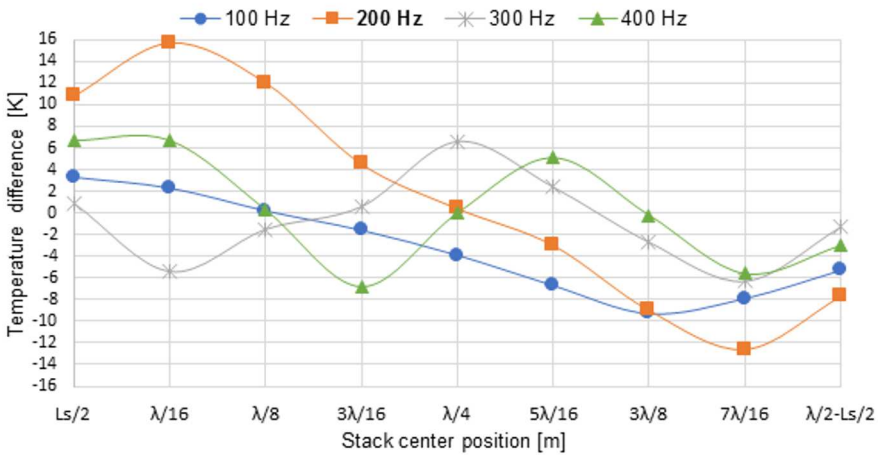

Figure 10: Temperature difference between stack ends versus stack position with main resonance frequency 200 Hz (λ is the wave length for 200 Hz).

The relations between the temperature difference and the stack position in the quarter-wave length resonator with two closed ends for 100 Hz and

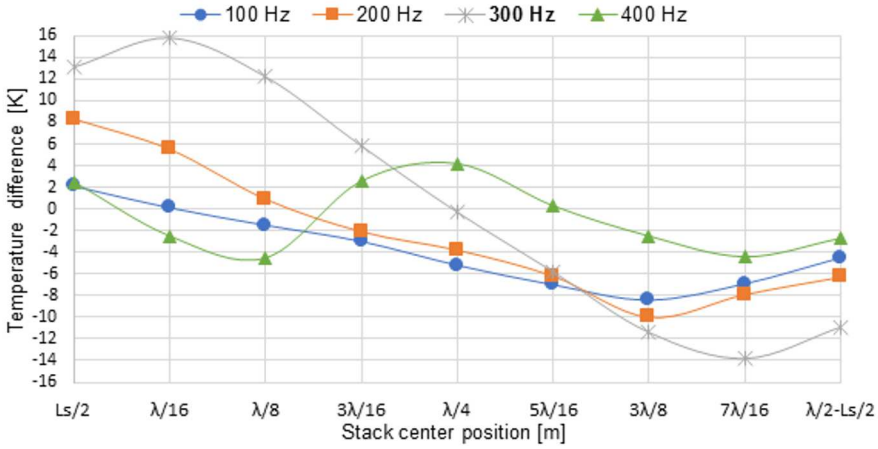

Figure 11: Temperature difference between stack ends versus stack position with resonance frequency 300 Hz (λ is the wave length for 300 Hz).

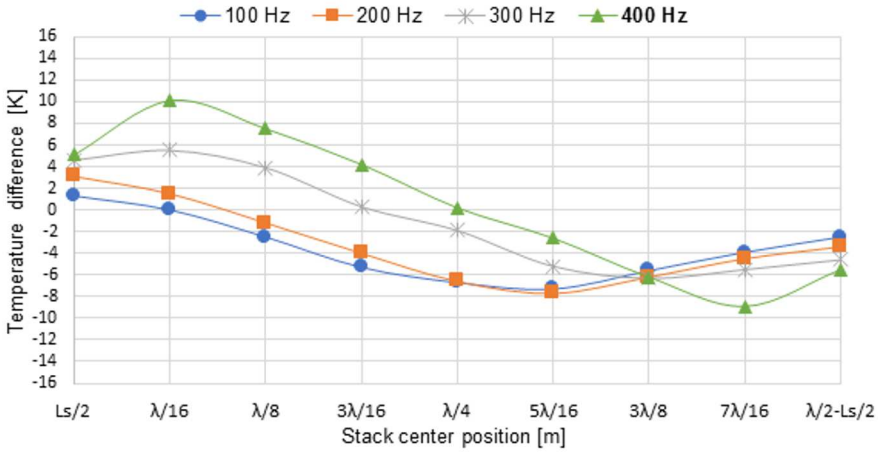

Figure 12: Temperature difference between stack ends versus stack position with resonance frequency 400 Hz (λ is the wave length for 400 Hz).

200 Hz are shown in Figs. 10 and 12. The temperature differences across the stack are lower than the results obtained for the half-wave length resonator. The acoustic wave in the quarter-length resonator with two closed ends is the combination of the incident wave and the wave reflected at the cork piston surface and thus the point at which heat transfer direction change

occurred. For the quarter-length resonator with one open end heat is always transferred in the same direction because the pressure node is located at the open end of the resonator. The temperature difference distributions for the resonator length other than quarter-wave length presented in Figs. 10–12 are also resulted from the mutual modification of the incident and reflected wave.

6 Conclusion

Theoretical and experimental investigations are carried out to examine the influence of stack position in the resonance tube and acoustic frequency on the performance of standing wave thermoacoustic refrigerator, which is measured in terms of the temperature difference produced at the ends of the stack. Nine different stack positions for four resonance frequencies with the half-wave length resonator were investigated. Additionally, the impact of other frequencies than resonance and the resonator length other than the half-wave was also checked.

The experimental results are in good agreement with the theory and confirm that stack position and acoustic frequency have significant effect on the operation of the thermoacoustic refrigerator. The highest temperature differences were obtained for resonance frequencies, resonator length corresponding to the half-length of acoustic wave, and the stack location at 1/16 of acoustic wave. The change in heat transfer direction always occurred at the pressure or velocity nodes. It was proved that the temperature difference across the stack is created also for other frequencies than resonance, but due to combination of the incident reflected wave the thermoacoustic effect is reduced.

Received 10 October 2017

References

[1] Herman C., Travnicek Z.: *Cool sound: the future of refrigeration technology? Thermodynamic and heat transfer issues in thermoacoustic refrigeration*. Heat Mass Transfer **42**(2006), 492–500.

[2] Grzebielec A., Rusowicz A., Laskowski A.: *Experimental study on thermal wave type adsorption refrigeration system working on a pair of activated carbon and methanol*. Chem. Process Eng-Inz **36**(2015), 4, 395–404, DOI: 10.1515/cpe-2015-0028

[3] Grzebielec A., Szelągowski A.: *Use of the water-silicagel sorption set in a refrigeration unit*. Przemysł Chemiczny **96**(2017), 2, 321–23, DOI:10.15199/62.2017.2.7.

[4] Xiao J. H.: *Thermoacosutic heat transportation and energy transformation. Part 1: Formulation of the problem*. Cryogenics **35**(1995), 1, 15–19.

[5] Swift G. W.: *Thermoacoustic engines*. J. Acoust. Soc. Am. **84**(1988), 4, 1145–1179.

[6] Babei H., Siddiqui K.: *Design and optimization of thermoacoustic devices*. Energ. Convers. Manage. **49**(2008), 3585–3598.

[7] Wetzel M., Herman C.: *Design optimization of thermoacoustic refrigerators*. Int. J. Refrig. **20**(1997), 1, 3–21.

[8] Tominga A.: *Thermodynamic aspects of thermoacoustic theory*. Cryogenics. 35(1995), 7, 427–440.

[9] Tijani M.E.H.: *Loudspeaker-Driven Thermoacoustic Refrigeration*. PhD thesis, Netherland University, Eindhoven 2001.

[10] Santillán A.O., Boullosa R.R.: *Space dependence of acoustic power and heat flux in the thermoacoustic effect*. Int. Commun. Heat Mass **22**(1995), 4, 539–548.

[11] Rulik S., Remiorz L., Dykas S.: *Application of CFD technique for modelling of the thermoacoustic engine*. Arch. Thermodyn. **32**(2011), 3, 175–190.

[12] Tijani M.E.H., Zeegers J.C.H., de Waele A.T.A.M.: *Design of thermoacoustic refrigerators*. Cryogenics **42**(2002), 49–57.

[13] Backhaus S., Swift G.: *New varieties of thermoacoustioc engines*. In: Proc. 9th Int. Con. on Sound and Vibration, 2002.

[14] Tijani M.E.H., Zeegers J.C.H., de Waele A.T.A.M.: *The optimal stack spacing for thermoacoustic refrigeration*. J. Acoust. Soc. Am. **112**(2002), 1, 128–133.

[15] Tijani M.E.H., Zeegers J.C.H., de Waele A.T.A.M.: *Construction and performance of a thermoacoustic refrigerator*. Cryogenics **42**(2002), 59–66.

[16] Herman C, Chen Y.: *A simplified model of heat transfer in heat exchangers and stack plates of thermoacoustic refrigerators*. Heat Mass Transfer **42**(2006), 901–917.

[17] Zolpakar N.A., Mohf-Ghazil N., El-Fawal M.H.:*Performance analysis of standing wave thermoascoustic refrigerator: A review*. Renew. Sust. Energ. Rev. **54**(20016), 626–634.

[18] Swift G.W.: *Thermoacoustic: a unifying perspective for some engines and refrigerator*. J. Acoust. Soc. Am. **113**(2003), 5, 2379–2381.

[19] Wetzel M., Herman C.: *Experimental study of acoustic effects on a single plate. Part I: Temperature fields*. Heat Mass Transfer **36**(2000), 7–20.

[20] Marx D., Mao H., Jaworski A.J.: *Acoustic coupling between the loudspeaker and the resonator in a standing-wave thermoacoustic device*. App. Acoust. **67**(2006), 402–419.

[21] Slaton W.V., Raspet R., Bass H.E., Lightfoot J.: *Working gases in thermoacoustic engines*. J. Acoust. Soc. Am. **105**(1999), 5. 2677–2684

[22] Tijani M.E.H., Zeegers J.C.H., de Waele A.T.A.M.: *Prandtl number and thermoacoustic refrigerators*. J. Acoust. Soc. Am. **112**(2002), 1, 134–143.